Exploring *in vivo* lesion myelination dynamics: Longitudinal Myelin Water Imaging in early Multiple Sclerosis

Hagen H. Kitzler [a,*], Hannes Wahl [a], Paul Kuntke [a], Sean C.L. Deoni [b], Tjalf Ziemssen [c], Jennifer Linn [a], Caroline Köhler [a]

[a] *Institute of Diagnostic and Interventional Neuroradiology, Carl Gustav Carus University Hospital, Technische Universität Dresden, Germany*
[b] *Department of Radiology, and Advanced Baby Imaging Lab, Warren Alpert Medical School at Brown University, Providence, RI, USA*
[c] *Center of Clinical Neuroscience, Multiple Sclerosis Center, Department of Neurology, Carl Gustav Carus University Hospital, Technische Universität Dresden, Germany*

A B S T R A C T

Background: Multiple Sclerosis (MS) lesions are pathologically heterogeneous and the temporal behavior in terms of growth and myelination status of individual lesions is highly variable, especially in the early phase of the disease. Thus, monitoring the development of individual lesion myelination by using quantitative magnetic resonance myelin water imaging (MWI) could be valuable to capture the variability of disease pathology and get an individual insight into the subclinical disease activity.

Objective: The goal of this work was (1) to observe the variation and longitudinal change of *in vivo* lesion myelination by means of MWI and its parameter *Myelin Water Fraction* (MWF), and, (2) to identify individual lesion myelination patterns in early MS.

Methods: In this study n = 12 patients obtained conventional MRI and quantitative MWI derived from multi-component driven equilibrium single pulse observation of T1 and T2 (mcDESPOT) within four weeks after presenting a clinically isolated syndrome and remained within the study if clinically definitive MS was diagnosed within the 12 months study period. Four MRI sessions were acquired at baseline, 3, 6, and 12 months. The short-term and long-term variability of MWF maps was evaluated by scan-rescan measures and the coefficient of variation was determined in four healthy controls. Tracking of individual lesions was performed using the *Automatic Follow-up of Individual Lesions* (AFIL) algorithm. Lesion volume and MWF were evaluated for every individual lesion in all patients. Median lesion MWF change was used to define lesion categories as decreasing, varying, increasing and invariant for MWF variation.

Results: In total n = 386 T2 lesions were detected with a subset of n = 225 permanent lesions present at all four time-points. Among those, a heterogeneous lesion MWF reduction was found, with the majority of lesions bearing only mild MWF reduction, approximately a third with an intermediate MWF decrease and highest MWF reduction in acute-inflammatory active lesions. A moderate negative correlation was determined between individual lesion volumes and median MWF consistent across all time-points. Permanent lesions featured variable temporal dynamics with the majority of varying MWF (58 %), however decreasing (16 %), increasing (15 %) and invariant (11 %) subgroups could be identified resembling demyelinating activity and post-demyelinating inactivity known from histopathology studies. Inflammatory-active enhancing lesions showed a distinct pattern of MWF reduction followed by partial recovery after 3 months. This was similar in new enhancing lesions and those with a non-enhancing precursor lesion.

Conclusion: This work provides *in vivo* evidence for an individual evolution of early demyelinated MS lesions measured by means of MWF imaging. Our results support the hypothesis, that MS lesions undergo multiple demyelination and remyelination episodes in the early acute phase. The *in vivo* MRI surrogate of myelin turnover bears capacity as a novel biomarker to select and potentially monitor personalized MS treatment.

1. Introduction

Multiple Sclerosis (MS) is characterized by the formation of perivenous inflammatory demyelinating lesions. The *in vivo* spatio-temporal dynamics of actively demyelinating and inactive lesions though is barely recognized.

Within newly forming MS lesions pro-inflammatory macrophages and activated CNS-resident microglia mediate a rapid focal demyelination by stripping off myelin from axons and the subsequent phagocytosis of myelin debris (Barnett et al., 2006; Henderson et al., 2009; Van Der Valk and De Groot, 2000; Yamasaki et al., 2014). With the lesion formation, an adaptive immune system propagation cascade of events excites and sustains this phagocytic demyelination (Lassmann et al., 2012; Wang et al., 2019).

Since focal inflammatory MS lesion myelin loss was found to be incomplete in autopsy samples, demyelination does not represent an irreversible process. As a matter of fact, rapid remyelination within actively demyelinating lesions was observed (Bramow et al., 2010;

Patrikios et al., 2006; Prineas et al., 1993; Raine and Wu, 1993). Such spontaneous remyelination within inflammatory MS lesions was found to be extensive in some MS patients possessing individually variable degrees of regeneration (Patrikios et al., 2006). It was therefore hypothesized that persistent inflammation in MS lesions may also simultaneously initiate tissue repair (Shechter and Schwartz, 2013). Besides this evidence of repair in early inflammatory active lesions even chronic MS lesions revealed remyelination (Chang et al., 2002).

Therefore, remyelination has become a therapeutic concept for tissue protection and repair in MS, whereby myelin regeneration targets the reduction of subsequent MS axonal injury and the disease-related disability caused by neurodegeneration (Franklin and Gallo, 2014; Reich et al., 2015). Thus, the development of monitoring tools is of utmost importance to provide individual *in vivo* selection criteria and to evidence therapeutic success.

Magnetic resonance imaging (MRI) provides a promising option to study lesion evolution *in vivo*. But limiting our comprehension of lesion myelination by means of clinical MRI series, the coexisting inflammation, demyelination and axonal loss in MS lesions cannot be differentiated *in vivo* by conventional sequences. The dynamic process of demyelination and eventual repair therefore can only indirectly be examined *in vivo* and remains poorly understood.

Within this pilot study we probed the myelin water imaging (MWI) method multi-component driven equilibrium single pulse observation of T1 and T2 (mcDESPOT) to investigate the dynamics of individual MS lesions immediately after clinical disease onset (Deoni et al., 2008). This technique allowed full brain coverage, 3D resolution, and, sufficient acquisition speed for clinically applied research. In addition, the stability of the respective quantitative measure Myelin Water Fraction (MWF) was investigated (Bouhrara et al., 2016; Deoni and Kolind, 2014). Finally, mcDESPOT was chosen for this study due to the advantage of whole brain quantification with high SNR efficiency (Alonso-Ortiz et al., 2015).

The aim of this study was (1) to observe the variation and longitudinal change of *in vivo* lesion myelination by means of MWI, and, (2) to identify possible individual lesion myelination patterns in longitudinal data at the initial stage of inflammatory active early MS.

2. Material and methods

2.1. Patient cohort and healthy control subjects

Clinical and imaging data of n = 12 patients were acquired within four weeks after presenting their first isolated neurological symptoms suggestive of underlying inflammatory central nervous system (CNS) disease and fulfilling the definition of a relapse (mean age 33.2 years (range 22–39); gender (M/F) 1:2). None of the patients received treatment at study baseline. Subsequently, two patients went on treatment with Copaxone at month 3 and one patient on Avonex at month 6. No patient received steroids during the study period.

The *Extended Disability Status Scale* (EDSS) and the *Multiple Sclerosis Functional Composite* (MSFC) were available at baseline and after 12 months with EDSS: 1.6 (0.4) and 1.5 (0.6) and MSFC 0.8 (0.3) and 1.0 (0.3) (mean (STD)), respectively. Data acquisition was part of an IRB approved study probing myelin imaging as a predictive biomarker of the conversion from the state of clinically isolated neurological syndromes to definite MS (Kitzler et al., 2018). As inclusion criterion for this study all patients had to be converted to clinically definite MS at the end of the study period (*re-evaluated after 9 months*).

As for probing the scan-rescan reproducibility of the applied myelin imaging method and the measurement variability within the observation period a healthy control (HC) group of n = 4 subjects (*mean age* 35.6 years (*range* 22–52); *gender* (M/F) 1:1.5) free of neurological diseases and a history of head trauma was also included. A greater healthy control group of n = 60 (*mean age* 39.7 years (*range* 20–79); *gender* (M/F) 1:1.8) was acquired for comparative measures.

The local institutional review board approved the source study and written informed consent was collected from all patients and healthy controls prior to data acquisition.

2.2. MRI acquisition

Myelin imaging and conventional MR imaging data were acquired at baseline, and after 3, 6, and, 12 months using a 1.5 Tesla scanner (*Magnetom Sonata, Siemens Healthineers, Erlangen Germany*) equipped with an 8-channel radio frequency head coil.

For the mcDESPOT protocol, sets of *fast low-angle shot* (FLASH) and *true fast imaging with steady state precession* (trueFISP) were acquired over a range of flip angles at constant echo time (TE), repetition time (TR), and inversion time (TI) using the following specifications: field of view (FOV) = 22 cm, image matrix = 128×128, slice thickness = 1.7 mm; FLASH: TE/TR = 2.0/ 5.7 ms, flip angle (α) = [5, 6, 7, 8, 9, 11, 13, 18]°; trueFISP: TE/TR = 1.71/3.42 ms, α = [9, 14, 19, 24, 28, 34, 41, 51, 60]°. The total acquisition time (TA) of theses mcDESPOT sequences was ~13 min.

An additional 3D resolved *Fluid-Attenuated Inversion Recovery* (FLAIR) scan (TE/TR = 353/6000 ms, TI = 2200 ms, FOV = 220×220 mm, image matrix = 256×210, slice thickness = 1 mm, TA = 5:50 min) was acquired to identify lesions. A T1-weighted 2D spin echo sequence (TE/TR = 500/90 ms, FOV = 187×250 mm, image matrix = 384×512, slice thickness = 3 mm, TA = 6:30 min) was acquired as anatomical reference and after injection of Gadolinium-DTPA (Gadolinium-diethylenetriaminepentaacetic acid; 0.1 mmol per kg body weight) to detect enhancement within acute inflammatory lesions.

2.3. MRI data processing including multicomponent relaxation data

The mcDESPOT data post-processing was executed by sets of in house developed python scripts to automate the *FMRIB Software Library* (FSL). MWF maps were calculated from the FLASH and trueFISP data for each time-point using the established mcDESPOT theory and processing method (Deoni et al., 2008). Initially *brain extraction* (BET) was performed (Smith, 2002) followed by an *intra-subject linear co-registration* using FLIRT (Jenkinson et al., 2002; Jenkinson and Smith, 2001) with 12° of freedom to the selected target (FLASH *image $\alpha = 18$°*).

Subsequently the registered series were fitted to the mcDESPOT algorithm to estimate the *two-compartment model* parameters of tissue water distribution for 1.5 T data (Deoni et al., 2008). The T1-weighted sequence was used as registration target. Registering every subsequent time-point of FLAIR data and MWF maps to the T1-weighted baseline scan allowed longitudinal analysis.

2.4. MWF intra-subject reproducibility

To estimate the intra-subject reproducibility of MWF a scan-rescan procedure within two weeks was performed in one healthy control subject. Further, three healthy control subjects were scanned and rescanned after 12 months to determine the reproducibility of MWF measurements within the study observation period. The mean MWF and standard deviation were determined in supratentorial WM to determine the *coefficient of variation* (CoV).

2.5. Longitudinal dummy lesion measurement variability

We further tested the longitudinal measurement variability within selected control WM *regions-of-interest* (ROI). Random ROI pairs (n = 40) were defined within contralaterally bihemispheric supratentorial WM locations representing variable sized dummy lesions typical for MS. ROIs were selected in (1) frontal, (2) parietal, (3) occipital, and, (4) temporal cerebral WM in both (a) periventricular and (b) subcortical locations free of gray matter or cerebrospinal fluid (CSF) partial volume effects. A volume range between 51 and 1051 mm^3 in plane volumes was

determined within every control subject at baseline and at 12 months.

A MWF variability threshold was estimated to determine the measurement bias for longitudinal MWF observations. Therefore, the *maximum MWF variability* within the selected lesion ROIs within the monitoring period was determined.

The ROI data dispersion was obtained using the *Bland-Altman* approach of determining the *mean differences* between the longitudinal measurements and the *'limits of agreement'*. The *Pearson correlation coefficient* of the measurements was calculated between the two time-points.

2.6. White matter T2 lesion segmentation

A semi-automatic method was used to generate binary masks of well-defined focal areas of elevated MRI signal intensity in FLAIR data as T2 WM lesions described elsewhere (Kitzler et al., 2012). The baseline lesion mask underwent a manual editing process by two independent readers, with long-term experience in MS imaging (*CK & HHK*). Further, every preceding mask was transferred to the subsequent time-point and manually re-edited with respect to new lesions and lesion size changes. FLAIR data were resampled to the slice thickness of the 2D T1 scan, yielding high in plane resolution with voxel spacing/resolution of $0.98 \times 0.98 \times 3$ mm and a voxel volume of 2.88 mm^3. For the longitudinal analysis only lesions of volumes >8.6 mm^3 (*equal to 3 voxels*) were incorporated into the lesion mask. Furthermore, to avoid CSF partial volume effects lesion voxels at the ventricles were discarded by correction of a dilated CSF mask (dilatation by 1 voxel).

2.7. Individual white matter T2 lesion tracking

An in-house developed lesion-tracking algorithm termed *Automatic Follow-up of Individual Lesions* (AFIL) was used to track volume and median MWF change of individual T2 lesions. This algorithm provided individual lesion volumes measured in mm^3 and considered different variants of T2 lesion evolution, i.e., *(a) new, (b) growing, (c) confluent, (d) separating, (e) stable, (f) shrinking, (g) vanishing, and (h) reappearing* lesions. As a result of six consecutive algorithm steps, AFIL found regionally corresponding T2 lesions within the provided time-series of segmented binary lesion mask (*see above*) by assigning *interim labels*. The subsequently found spatial intersection of *interim labeled* lesions between the baseline and the follow-up time-point allowed the forward identification of *connected interim lesion labels* in consecutive time-points. Finally, a *global label* was assigned to these *connected interim lesion labels*. This allowed tracking the same individual lesion within the entire time-series by the same *global label*. We refer to the original description for more detailed information regarding the algorithm (Köhler et al., 2019).

Integrating the dynamics of individual lesion volume change between all study time-points the algorithm results were further specified to retrieve categories of longitudinal development, as (1) *varying*, (2) *growing*, (3) *stable*, (4) *shrinking individual T2 lesion volumes, and,* (5) *resolving*, i.e., shrinkage below the limit of detection and (6) *reappearing lesions*.

Based on the AFIL label *permanent and new lesions* were selected for subsequent measurement analyses. This allowed determining the variation of volumes and MWF values.

The MWF changes of Gad-enhancing lesions with a precursor, i.e. lesions non-enhancing in a prior MRI but enhancing at a later time-point, and new enhancing lesions were further observed separately. Non-enhancing new lesions and lesions that enhanced at baseline were excluded.

2.8. Determination of individual white matter T2 lesion MWF

The AFIL algorithm generated *globally labeled lesion masks* that were used as ROI within co-registered MWF maps to determine and monitor the subsequent individual lesion median MWF, *standard deviation* (STD) and *inter-quartile range* (IQR) for every lesion.

2.9. Statistical analysis

Statistical analysis was performed using MATLAB *Statistics Toolbox*. *Pearson correlation coefficients* were obtained between the individual ROI measurements. *Coefficient of variation* (CoV) mapping for MWF was performed. The *Bland-Altman analysis* and plotting was conducted using an individual python script. A pairwise *Spearman rank correlation* analysis was applied to lesion volume and lesion median MWF. The Pearson's correlation coefficient was determined and a paired *t-test* was applied to HC dummy lesion measurements within the monitoring period.

3. Results

3.1. MWF intra-subject reproducibility and longitudinal ROI variability

The short-term scan-rescan acquisition within two weeks representing the intra-subject reproducibility of MWF provided a CoV of 4.3 %. The long-term follow-up scan interval equal to the study period of 12 months revealed a CoV of 3.5 % (range 2.7–4.3 %) of the comparison of entire WM mean MWF across healthy controls (Fig. 1).

3.2. Measurement variability of dummy lesions

The analysis in regional lesion-sized control WM ROIs (i.e. *MS lesion simulation*) revealed a baseline median MWF of 0.259 ± 0.003 and a median MWF of 0.258 ± 0.004 of the re-scan at the end of the observation period for all ROI volumes collectively.

All longitudinal measurements did not differ significantly (*t-test; p-value 0.094*). Furthermore, the *Pearson correlation coefficients* between the correspondent individual ROI measurements demonstrated that the median MWF values were highly correlated within single subjects (*mean r = 0.93*) equal to an intra-subject homogeneity of MWF measures.

The *Bland-Altman Analysis* of longitudinal ROI measurements using a 95 % confidence interval indicated a low bias between the baseline and the re-scan at the end of the observation period (Fig. 2). The mean MWF difference between the two measurements was 0.001, the *upper limit* was 0.004 and the *lower limit* -0.003 for all ROIs. A conservative threshold of lesion median MWF change of ± 0.01, i.e. greater than two standard deviations and the maximum variability of MWF difference, was chosen to subsequently define relevant MWF change and the myelination lesion categories (*see section 3.2*).

We defined a MWF change < -0.01 as a MWF decreasing lesion and >0.01 as MWF increasing lesion in contrast to a change ≤ 0.01 in MFW between two observations.

3.3. Longitudinal quantitative observation of MS lesions

3.3.1. Individual white matter T2 lesion tracking

We tracked a total of n = 386 T2 lesions segmented within FLAIR data which were globally labeled by the AFIL algorithm. A subset of n = 225 permanent lesions (58.3 %) was present at all four time-points of observation, and n = 127 new lesions (32.9 %) were longitudinally tracked. Hence, resolving (n = 23) and reappearing (n = 11) lesions were excluded from further analysis. Resolving and reappearing lesions were smaller than 23 mm^3.

An example case of the evolution of AFIL labeled *lesions* including their subsequent measurement is illustrated in Fig. 3 demonstrating the highly variable individual lesion development.

The baseline lesion inspection revealed disparities in median MWF decrease. The relative MWF decrease within lesions was assessed using a trisection of the healthy control WM median MWF (0.23). Lesional MWF decrease was categorized as severe if MWF was found <0.08,
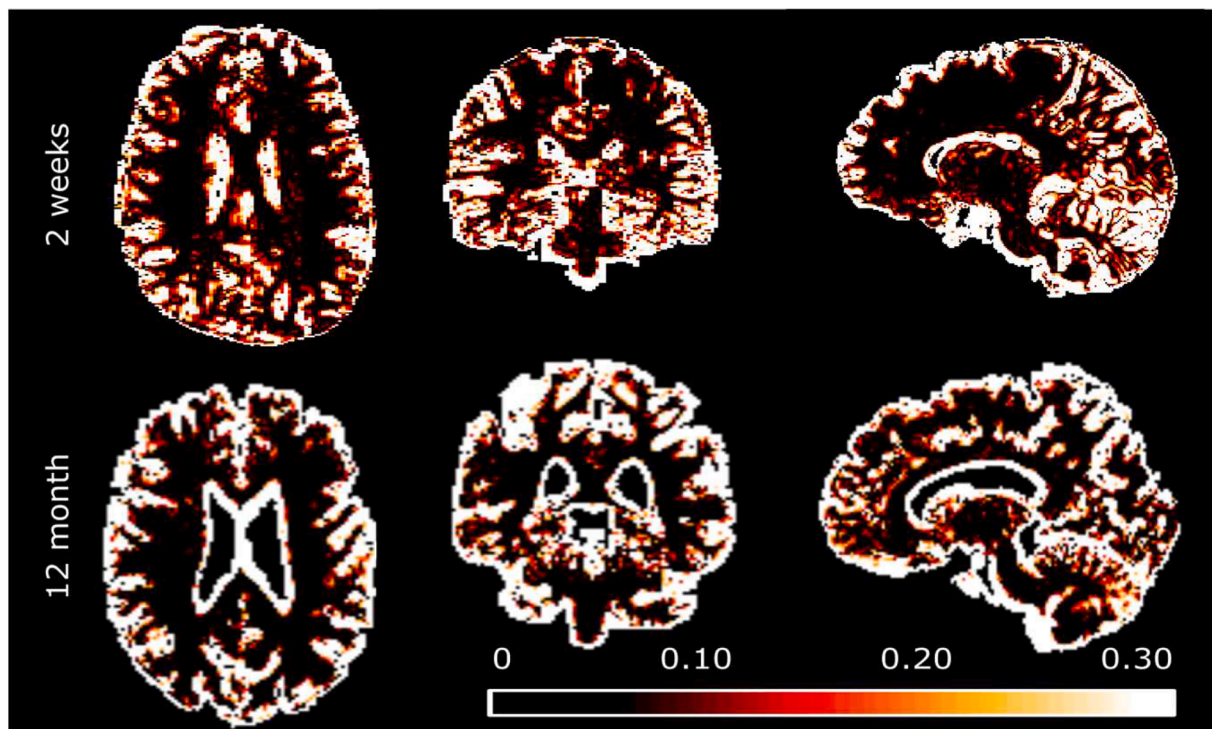
Fig. 1. CoV (*coefficient of variation*) maps for healthy control MWF. **Top row**: Short-term scan-rescan procedure CoV displayed in axial, coronal and sagittal exemplary slices. **Bottom row**: The CoV of the long-term follow-up measurement within the study period of 12 months. Within both analyses the CoV was consistently below 5 % in cerebral and cerebellar white matter but considerably higher in cerebral grey matter. A notably higher CoV was found in subependymal location at ventricular boundaries (*Note that two different control subjects are displayed*).

intermediate with values of $0.08 \leq MWF \leq 0.16$, and, mild if MWF was >0.16. As a result the majority of n = 155 (69 %) of lesions revealed mild MWF decrease, whereas n = 68 (30 %) lesions had an intermediate reduction and only n = 2 (1 %) lesions featured a severe decrease of MWF values.

3.3.2. Individual MWF and volume development of permanent lesions

The permanent lesions were categorized to further analyze the heterogeneity of MWF development. Therefore, lesion categories were assigned based on their overall MWF development within the observation period. Lesion groups of 1) *decreasing* (*suggestive of demyelination*) and 2) *increasing* MWF (*suggestive of remyelination*) were distinguished from 3) *varying* MWF lesions with variable decrease and increase in MWF. Finally, all lesions with MWF change ≤ 0.01 were assigned to 4) *invariant* MWF lesions. (Fig. 4). The MWF within permanent lesions ranged from not relevant up to >90 % reduction from healthy WM with a median of 28.6 %.

For comparison of lesion MWF and volume development the quantitative categories 1) *decreasing* (*shrinkage*), 2) *increasing* (*growth*), 3) *varying* and 4) *invariant* lesion volume were similarly introduced based on a volume threshold of 3 voxels (8.6 mm³).

The permanent lesion cohort revealed n = 130 lesions with longitudinally varying MWF, n = 37 with continuous MWF decrease, n = 33 with permanent MWF increase and n = 25 with invariant MWF over the study period of 12 months (Fig. 5A).

The lesion volume change within the permanent lesion cohort was varying in n = 171 lesions, increasing in n = 7, decreasing in n = 3, and invariant in n = 38 (Fig. 5B).

The individual MWF development within the evolution subgroups was determined. Within a lesion time series comparison of MWF medians (Fig. 6; A-D) the median of decreasing MWF lesions reached a value (A; 12 months) similar to the steady median of varying MWF lesions (B) and in turn this value and the initial median of increasing MWF lesions (C; 0 months) were alike. Beyond that, the MWF increase reached

a median value and distribution (C; 12 months) very similar to that of invariant MWF lesions (D).

The corresponding volume changes in permanent lesion MWF evolution subgroups were determined (Fig. 6; E-H). The majority of lesions revealed volumes lower than 150 mm³ and lesions with highest volumes were found in the varying MWF category. However, MWF invariant lesions revealed the lowest median volume (H).

A moderate negative correlation was determined for the volume of individual lesions and their median MWF for all measurement timepoints (r_1 = -0.43, p < 0.001; r_2 = -0.44, p < 0.001; r_3 = -0.45, p < 0.001; r_4 = -0.42, p < 0.001).

Further, a positive correlation was found for lesion volume and the IQR of the related MWF within the lesion at all four study measurements time-points (r_1 = 0.64, p < 0.001; r_2 = 0.64, p < 0.001; r_3 = 0.64, p < 0.001; r_4 = 0.66, p < 0.001).

3.3.3. Individual MWF development of gadolinium enhancing lesions

Lesions with Gadolinium enhancement representing an acute inflammatory T2 lesion group were separately explored. Here newly appearing enhancing (n = 25) and enhancing lesions with a non-enhancing precursor (n = 12) were distinguished (Fig. 7).

Enhancing lesions with a precursor, i.e. lesions non-enhancing in a prior MRI but enhancing at a later time-point, and new enhancing lesions showed a variable MWF drop with a median reduction at the time-point of enhancement to approximately 50 % MWF of that of NAWM. Further, the median MWF in both lesion types at the time-point of enhancement (adjusted month 0) was lower than the median MWF of all other permanent lesion categories (see Fig. 6). Both lesion types, i.e. new enhancing lesions and re-enhancing lesion with a precursor, thereinafter featured a net increase of MWF within 3 months after enhancement.

4. Discussion

Inflammatory demyelination is the key target to be modulated by
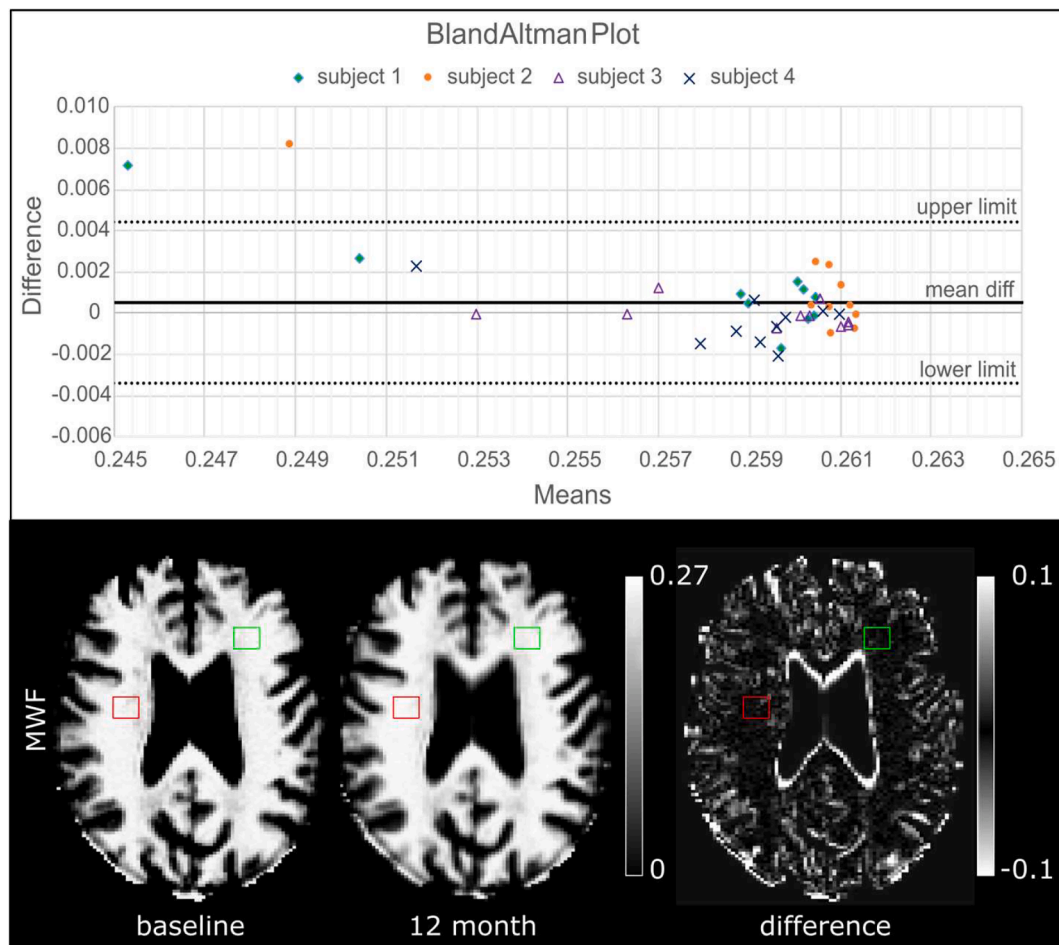
Fig. 2. The *in vivo* repeatability of MWF measurement of lesion-sized healthy WM ROIs at *baseline* and follow-up. *Top*: *Bland-Altman Plot* displaying the differences of the individual ROI MWF medians of the two longitudinal measurements against their mean. Whereas the majority of the ROI measurements were located within the 95 % *'limits of agreement'* (i.e. the mean of the two values, ±1.96 standard deviations) two ROIs (*stacked dots*) provided a maximum difference of 0.008 in median MWF outside the limits. *Bottom*: Example illustration of the origin of the measurements. MWF baseline and 12 months maps displaying example ROIs in cerebral WM and their associated difference map.

disease-modifying treatments in early MS. In addition to estimate new and enlarging WM lesions as marker for subclinical disease activity, it is important to understand the severity of myelin loss of individual MS lesions and whether repair processes take place over time. Therefore, we probed the MWI method mcDESPOT and its derived parameter MWF in this study as an *in vivo* tool to monitor changes in myelin content in a group of patients with early MS within the first year after diagnosis of clinically isolated syndromes.

We applied the lesion tracking method to automatically record the longitudinal quantification of individual lesion metrics from advanced MRI techniques. (Köhler et al., 2019). The executed scan-rescan analyses revealed reliable repeated MWF measurements in lesion-size sub-volumes of brain WM.

The determined mean CoV of 4.3 % throughout healthy control WM of our study was comparable to other mcDESPOT studies at the similar field strength that reported a CoV between 3.8 and 7.0 % for MWF in different WM regions (Deoni et al., 2009; Kolind et al., 2012). In addition the retrieved long-term CoV of 3.5 % proofed to be comparable to short-term measures, indicating highly reproducible MWF measures in WM.

Investigating our baseline data immediately after diagnosis of an inflammatory CNS disease we found a heterogeneous lesion MWF reduction. Whereas the majority (69 %) of WM lesions revealed only a mild MWF reduction approximately a third of the lesions showed an intermediate MWF decrease. Substantial lesion MWF reduction was a

rare finding. This is comparable to the findings of Prineas et al. that found 39 % demyelinating lesions, 22 % partially remyelinated lesions and completely demyelinated lesions absolutely rare in histopathology of 15 patients with 2.5 to 18 months after disease onset (Prineas et al., 1993). In contrast Schmierer et al. reported 87.0 % lesions to be demyelinated and 13.0 % remyelinated in histopathology of 20 studied MS subjects but with long-term disease duration of mean 29.5 years (Schmierer et al., 2004). These results allow only restricted comparison since selective subsets of individual lesions were sampled in contrast to our whole-brain approach. However, differences can be explained by remyelination capacity impairment in chronic disease (Goldschmidt et al., 2009; Kuhlmann et al., 2008).

In this study larger lesions revealed a higher degree of MWF reduction than smaller lesions at baseline and permanently over the study period based on persistent negative correlations between lesion volume and MWF. This reflects an invariance of the pattern of lesion myelination changes in early MS. Furthermore, small lesions showed a more homogeneous MWF decrease and larger lesions showed a heterogeneous MWF distribution based on the correlation of lesion volume and IQR of the associated MWF within the lesion. Given the small volume of lesions in relation to lower clinical image resolution here, careful interpretation needs to include causative partial volume effects. However, alternatively this could mirror lesion remyelination besides incomplete demyelination. In fact high resolution *ex vivo* imaging and histopathology found lesions fully remyelinated or partly remyelinated at the edge of an
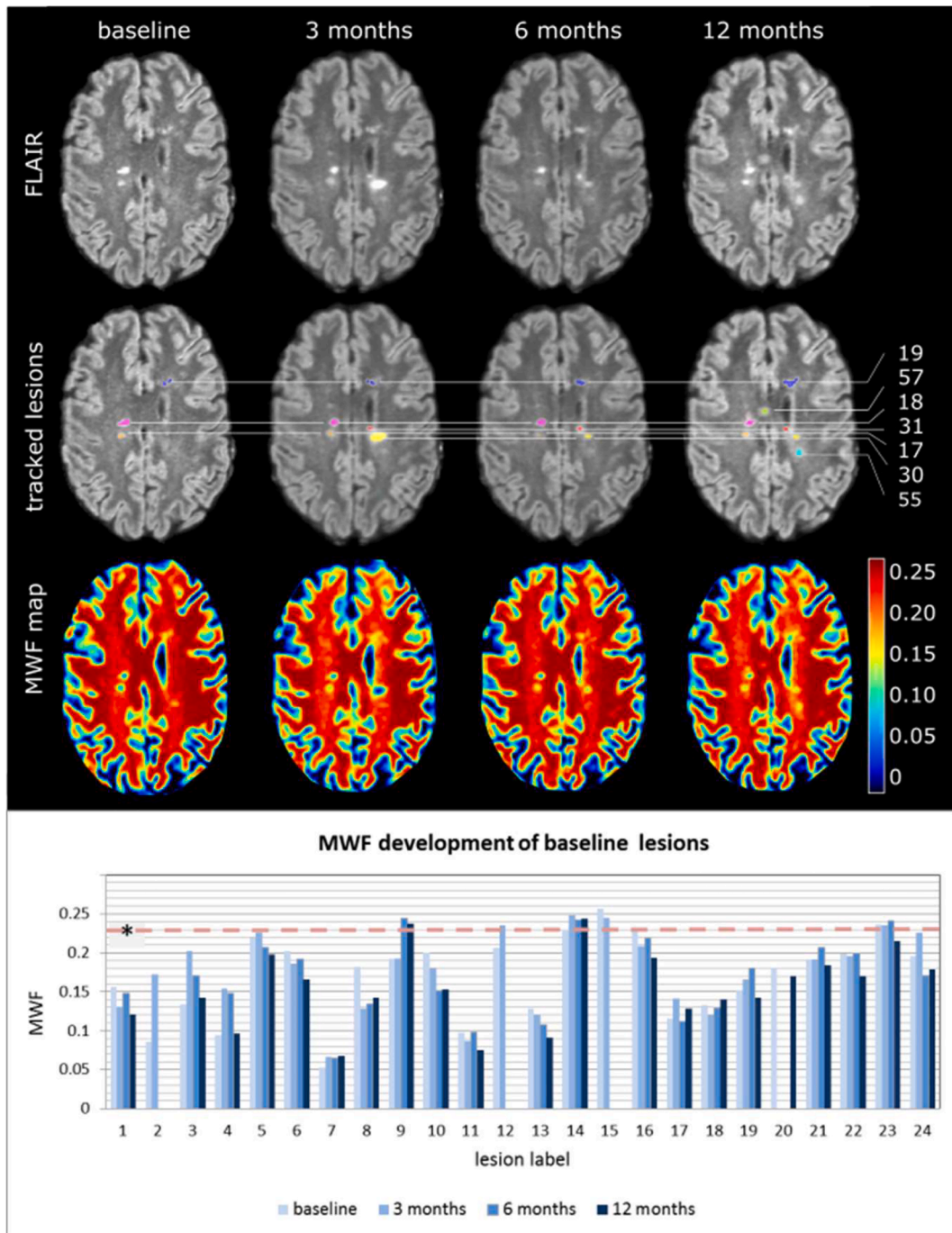
Fig. 3. Example of an individual MS patient MRI study time series. **First row**: Registered FLAIR axial reformations from the four study MRIs display lesion load in this slice at the different time-points. **Second row**: FLAIR and AFIL labeled lesion mask. Each lesion is coded with an individual color, kept constant throughout the four study time-points. Baseline lesions # 17, 18 and 19 represent permanent lesions visible in this slice (*connecting line*), while lesions # 30, 31, 55, 57 are new lesions after 3 (#30, 31) and 12 (#55, 57) months, respectively. **Third row**: Color-coded Myelin-Water-Fraction (MWF)-map of the same slice demonstrating MWF baseline status and MWF development of those lesions over time. **Bottom section**: The MWF development of all 24 T2 lesions existing at baseline in this patient is displayed in a bar graph with values of all four time-points per lesion. The healthy control median MWF in WM is marked (* median MWF $_{healthy\ controls}$ = 0.23; IQR = 0.039). This exemplary case demonstrates a median reduction of MWF within the majority of T2 lesions. A minor subset of lesions revealed MWF levels comparable to MWF of healthy control WM (Fig. 3 lesion # 9, 14, 15, 23). Moreover, lesions of low volumes < 0.20 ml resolved (# 2, 12, 15) and reappeared (# 20) in this example patient; assumedly because of small size at the detection limit or/and volume changes. Whereas most lesions revealed variable MWF values over time, here lesion 13 showed a permanent loss in MWF.

otherwise centrally demyelinated lesion (Barkhof, 2003; Brück and Stadelmann, 2003; Schmierer et al., 2004).

The *in vivo* individual MWF lesion tracking allowed monitoring a spectrum of temporal dynamics. We observed four different courses of lesion development whereas the largest proportion of lesions featured a varying MWF with alternating decrease and increase equal to demyelinating and remyelinating activity. This is consistent with the results of histopathological studies that have identified inflammatory active demyelinating lesions as the most frequently found lesion type in very early MS of disease duration ≤ 1 year (Frischer et al., 2009) and in
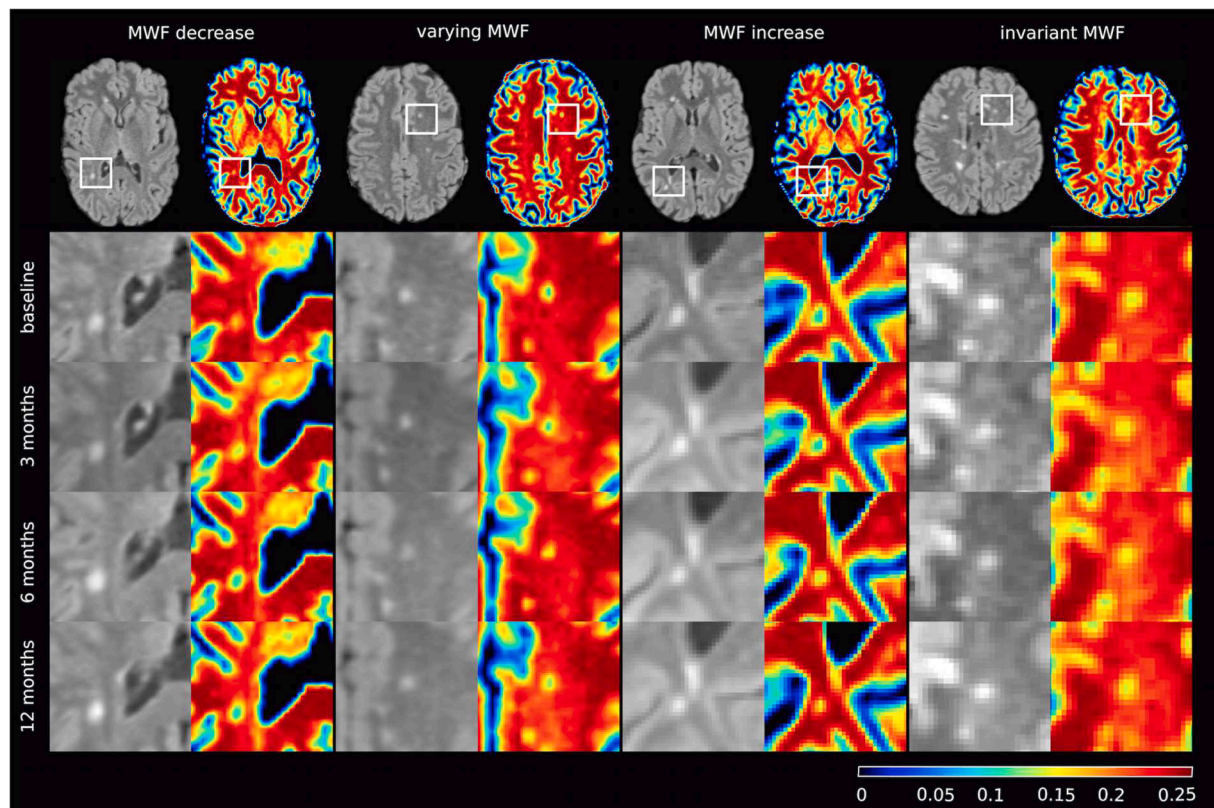
Fig. 4. Lesion development categories in the course of four consecutive MRIs (four different cases): Selected FLAIR slice of the observed baseline lesion and its corresponding MWF map (*first row*); frame inserts in the FLAIR slice represent zoomed regions vertically tabulated below as baseline, 3, 6, and, 12 months corresponding sections (*row 2–5*). Longitudinal analysis of lesion MWF revealed (1) decreasing, (2) varying, (3) increasing, or, (4) invariant median MWF values within the lesions.

established MS patients with short disease duration (Kutzelnigg, 2005).

The extent of imaging *in vivo* measurable myelin loss assumedly reflects a net effect of simultaneous myelin loss and regain. This is reflected by the tremendous MWF distribution in active varying MWF lesions in our study suggesting that the effects of both paralleled processes are depicted at certain stages. The further found 15 % lesions with continuous MWF increase mirror the results of histopathology studies that revealed extensive remyelination in approximately 20 % of individual lesions in MS (Goldschmidt et al., 2009; Patani et al., 2007; Patrikios et al., 2006).

However, to date no uniform pathological WM lesion classification nor sufficiently verified concept of their dynamics in MS exists. Proposals for such a histological system are based on inflammatory and demyelinating activity. Referring to histopathology, Kuhlmann et al. proposed a division into (1) active, (2) mixed active/inactive and (3) inactive lesions based on ongoing demyelination, with subdivision off 1 and 2 into demyelinating and post-demyelinating lesions. In addition active lesions were further subdivided into early and late demyelination based on histopathology and immunohistochemistry features (Kuhlmann et al., 2016).

In reflection of this comparative classification, our analysis based on dynamic MWF categories (Fig. 6) suggested temporary pattern of active and mixed active/inactive lesions based on MWF changes (decreasing-varying) towards inactive lesions (increasing-invariant) with finally stable MWF. Strikingly *demyelinating activity* and *post-demyelinating inactivity* resemble the varying MWF characteristics found in this study with continuous MWF decrease representing constantly active demyelinating lesions (Fig. 6A) within the observation period. The transient increase of lesion MWF within the varying lesion group (Fig. 6B) may here correspond to an interim post-demyelinating lesion status according to the Kuhlmann classification and potentially intermediate myelin

repair. Alternatively, it may illustrate early and late demyelination in decreasing and varying groups, respectively. Finally, the increasing and invariant MWF lesion groups (Fig. 6C + 6D) of this study may represent a post-demyelinating status with constant remyelination up to demyelinating inactivity.

A part of the lesions featured an invariant MWF indicating a stable myelination. Within this group, some lesions showed a higher MWF decrease suggesting a sustained demyelination or very poor recovery. In addition, another group of lesions with a persistent increase in MWF was found, indicating higher remyelination activity.

There is *in vivo* evidence of repeated episodes of demyelination and remyelination (*'first hit' and 'second hit' theory*) and different rounds of demyelination in MS lesions (Brown et al., 2014). Within our small subgroup observation of new enhancing lesions and enhancing lesions with a non-enhancing precursor the median MWF in both groups deviated from permanent non-enhancing lesions with the overall lowest MWF values. Although a lower capacity to repair and thus lower myelin recovery was expected after more than one hit our subgroups revealed a similar reduction at the time-point of enhancement and a MWF recovery after 3 months especially in lesions with a precursor (Fig. 7). The latter is in accordance with Vargas et al. that probed MWF in new enhancing MS lesions and after 2 to 12 months follow-up and found significant MWF improvement (Vargas et al., 2015). However, the finding of lesser recovery in enhancing lesions with a precursor in comparison to new lesions by Brown et al. was not replicated. In contrast to our early MS cohort Brown et al. examined lesions in RRMS and secondary-progressive MS (SPMS) with disease durations >7 years presumably leading to this disagreement (Brown et al., 2014). The myelin recovery may be preserved in very early disease. However, due to the limited number of enhancing lesions in our study and the lack of appropriate statistics, respective interpretations of these result should be treated

A - Early MS lesion MWF development
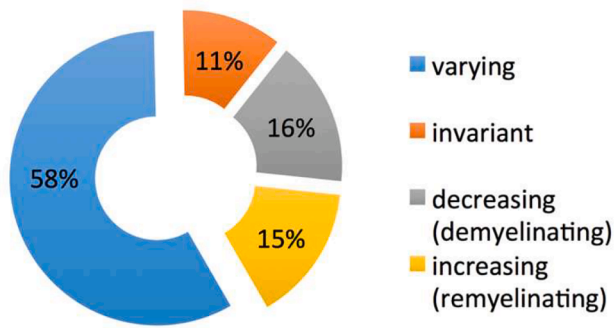
B - Early MS lesion volume development
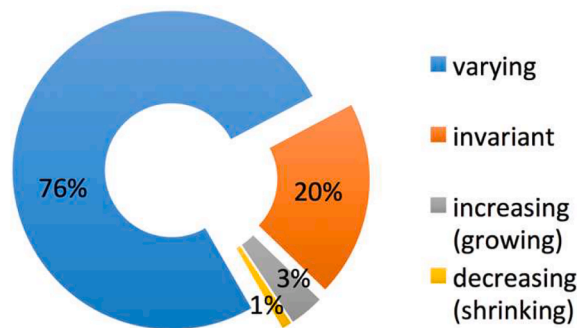
Fig. 5. Distribution of permanent early MS lesion categories based on multiple longitudinal measurements. The lesion MWF net change (A) and overall lesion volume development (B) lesion categories after a 12 months period of early MS are provided as percentages. Note that (in contrast to Fig. 6) here categorization for an individual lesion was independent from the respective measurement of volume or MWF. (The similar color coding of decreasing MWF and increasing volume and vice versa was chosen based on an assumed relation of lesion growth and demyelination and lesion shrinkage and remyelination, respectively).

with caution.

Distinct histopathology and immunohistochemistry features to specify MS lesion tissue changes are far beyond MRI capability. However, MRI can provide *in vivo* pathology with the tremendous benefit of repeatability and the acquisition of longitudinal dynamics. Quantitative MRI measures however are prone to errors due to additional tissue alterations and our study may hence have some limitations.

In this pilot study we did not correct for the total water content. The parameter MWF is a fraction of water signal trapped between myelin bilayers to total water content. An increase in water content for example due to edema could result in lower MWF values. Within our analysis inflammatory edema in acute lesions and a change of intracellular and extracellular water content due to tissue destruction and axonal loss could have influenced the precision of MWF quantification. In awareness of this uncontrollable imprecision the minor number of lesions (1 %) with very low MWF values ≤ 0.1 suggestive of severe demyelination could also have been acute edematous lesions. However, Vavasour and colleagues recently stated that water content changes in new MS lesions have a minimal effect on the determination of myelin water fraction values (Vavasour et al., 2021). In this respect a treatment effect of immune-modulating therapies on lesion water content also needs to be considered when monitoring treated MS patient cohorts. In this study such initial effects may have had an impact on MWF change of lesions on the three patients that received therapy initiation during the study period.

Another important fact is that mcDESPOT may be affected by magnetization transfer effects and tissue iron content influencing the precision of MWF quantification (Zhang and MacKay, 2013).

Further the ground truth derived from human evaluation of lesion tissue may have been limited in precision of lesion border selection although lesions were carefully segmented and manually edited by two experienced raters. However, the distinction of perifocal edema around acute inflammatory lesion provides a challenge and may have influenced some lesion segmentation result.

Finally the hereby applied *two-compartment model* analysis of mcDESPOT only acts on the assumption of intra/extracellular and myelin water but does not take into account the influence of propagating inflammatory cells. This effect has not yet been properly addressed.

Our findings demonstrate an *in vivo* measurable, highly dynamic individual lesion myelination status in patients immediately after the diagnosis of clinically isolated syndrome and subsequent early MS diagnosis. The used technology and analysis method facilitate to quantify WM lesion formation and to observe damage and reparative mechanisms. This may allow depicting phenotypes of the extent of myelin loss and its dynamic myelination features to select patients for individualized therapeutic approaches and to monitor their remyelination response.

Since the patients assessed in this study were a selected subset of early MS patients with a short time to conversion to clinically definite MS, they were therefore likely to exhibit a more aggressive disease course. Our findings for this reason may not be generalized to later stages of the disease and the small number of patient observed in this study even more limits generalizability. Further research will need to address lesion MWF differences in established RRMS and SPMS in greater cohorts in comparison to clinical data. Research applications may involve long-term lesion evolution assessments probing detailed monitoring of the heterogeneous disease progression of MS patients.

5. Conclusion

This work provides *in vivo* evidence for a non-uniform demyelination evolution of early MS lesions measured by means of MWF imaging. Our results support the hypothesis, that MS lesions undergo multiple demyelination and remyelination episodes in the early acute phase (Prineas et al., 1993; Brown et al., 2014). The presented longitudinal measurements further illustrate a high variance of the short-term relative myelin content of individual MS lesions within subjects.

Our results demonstrated the capability of the analysis algorithm to differentiate lesion evolution stages in individual patients *in vivo*. The implemented procedural method allowed uncovering an unacquainted dynamic aspect of early MS inflammatory demyelination of clinical diagnostic potential and the derived myelination alteration categories can be exploited as individual patient myelination fingerprints. Hence serial MWF imaging and analysis in pre-therapy early MS may enable to estimate individual disease severity based on the degree of demyelination and remyelination capacity.

Clinical applications may allow quantifying the demyelinating burden of disease and demyelinating activity in MS, to differentiate between fast and slow inflammatory MS phenotypes and determining individual intrinsic remyelination capacity. The latter may have important implications for addressing potential candidates for remyelination-inducing therapies. In summary the hereby-quantified *in vivo* MRI surrogate of myelin turnover bears capacity as a novel biomarker to select and potentially monitor personalized MS treatment.

CRediT authorship contribution statement

Hagen H. Kitzler: Conceptualization, Methodology, Project administration, Investigation, Supervision, Writing – original draft. **Hannes Wahl:** Data curation, Software. **Paul Kuntke:** Data curation, Formal analysis, Software. **Sean C.L. Deoni:** Resources, Software, Data
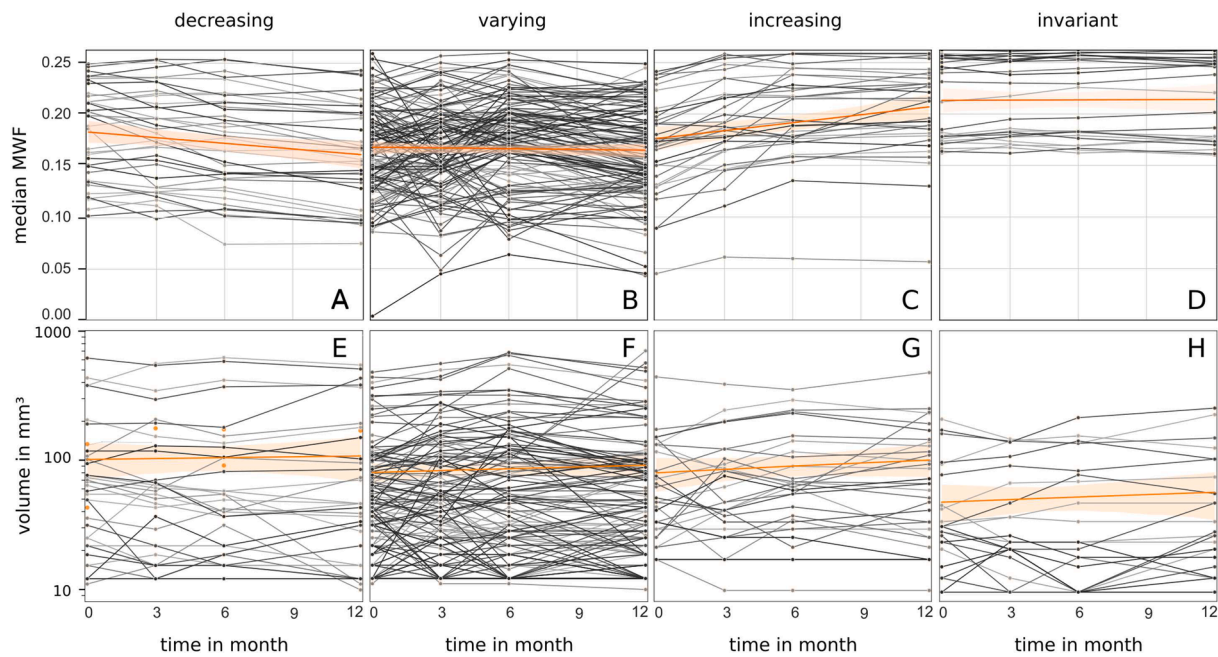
Fig. 6. Time series of permanent lesion median MWF in distinct decreasing, varying, increasing and invariant MWF categories (A-D). For comparison the corresponding lesion volume courses are provided in subjacent plots (E-H). Here the lesion volume development was selectively plotted for the MWF category cohort for direct comparison. The category median respective value regression and the 95% confidence interval are included (*orange line and transparent area*).
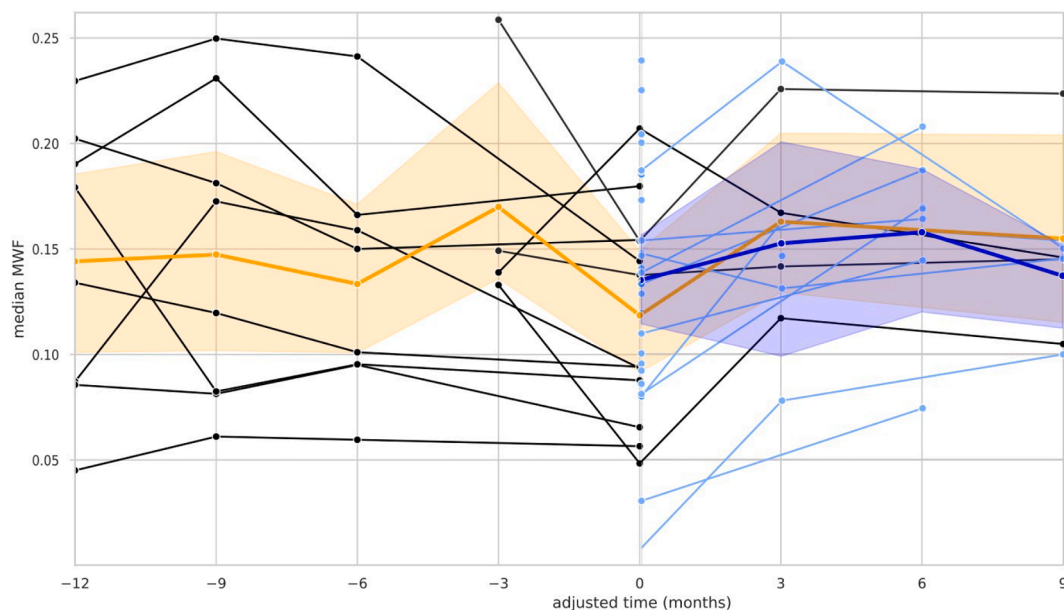
Fig. 7. MWF development in Gadolinium enhancing new lesions (*blue lines*) and re-enhancing lesions with a non-enhancing precursor (*black lines*). For comparison of the subsequent MWF development the time series was adjusted for all lesions to appear at time-point $> 0 <$ when Gadolinium enhancement was present. The median and the 95 % percentile interval are included (the median as an orange line and a transparent interval area for enhancing lesions with precursor; dark blue line and transparent area for the new enhancing lesion respectively).

curation. **Tjalf Ziemssen:** Resources. **Jennifer Linn:** Supervision. **Caroline Köhler:** Project administration, Software, Visualization, Investigation, Validation, Writing – review & editing.

Declaration of Competing Interest

The authors declare that they have no known competing financial interests or personal relationships that could have appeared to influence the work reported in this paper.

Data availability

The authors do not have permission to share data.

References

Alonso-Ortiz, E., Levesque, I.R., Pike, G.B., 2015. MRI-based myelin water imaging: a technical review. Magn. Reson. Med. 73, 70–81.

Barkhof, F.B.W., De Groot, C.J., Bergers, E., Hulshof, S., Geurts, J., Polman, C.H., van der Valk, P., 2003. Remyelinated lesions in multiple sclerosis: magnetic resonance image appearance. Arch Neurol. 60, 1073–1081.

Barnett, M.H., Henderson, A.P., Prineas, J.W., 2006. The macrophage in MS: just a scavenger after all? Pathology and pathogenesis of the acute MS lesion. Multiple Sclerosis J. 12, 121–132.

Bouhrara, M., Reiter, D.A., Celik, H., Fishbein, K.W., Kijowski, R., Spencer, R.G., 2016. Analysis of mcDESPOT- and CPMG-derived parameter estimates for two-component nonexchanging systems. Magn. Reson. Med. 75, 2406–2420.

Bramow, S., Frischer, J.M., Lassmann, H., Koch-Henriksen, N., Lucchinetti, C.F., Sorensen, P.S., Laursen, H., 2010. Demyelination versus remyelination in progressive multiple sclerosis. Brain 133, 2983–2998.

Brown, R.A., Narayanan, S., Arnold, D.L., 2014. Imaging of repeated episodes of demyelination and remyelination in multiple sclerosis. Neuroimage Clin 6, 20–25.

Brück, W.K.T., Stadelmann, C., 2003. Remyelination in multiple sclerosis. J. Neurol. Sci. 15 (206), 181–185.

Chang, A., Tourtellotte, W.W., Rudick, R., Trapp, B.D., 2002. Premyelinating oligodendrocytes in chronic lesions of multiple sclerosis. N. Engl. J. Med. 346, 165–173.

Deoni, S.C.L., Kolind, S.H., 2014. Investigating the stability of mcDESPOT myelin water fraction values derived using a stochastic region contraction approach. Magn. Resonance Med.

Deoni, S.C.L., Rutt, B.K., Arun, T., Pierpaoli, C., Jones, D.K., 2008. Gleaning multicomponent T1 and T2 information from steady-state imaging data. Magn. Reson. Med. 60, 1372–1387.

Deoni, S.C., Samson, R., Wheeler-Kingshott, C.A.M., 2009. Intra and inter-site reproducibility of myelin water volume fraction values derived using mcDESPOT. Proc. Intl. Soc. Mag. Reson. Med. 17.

Franklin, R.J., Gallo, V., 2014. The translational biology of remyelination: past, present, and future. Glia 62, 1905–1915.

Frischer, J.M., Bramow, S., Dal-Bianco, A., Lucchinetti, C.F., Rauschka, H., Schmidbauer, M., Laursen, H., Sorensen, P.S., Lassmann, H., 2009. The relation between inflammation and neurodegeneration in multiple sclerosis brains. Brain 132, 1175–1189.

Goldschmidt, T., Antel, J., König, F.B., Brück, W., Kuhlmann, T., 2009. Remyelination capacity of the MS brain decreases with disease chronicity. Neurology 72, 1914–1921.

Henderson, A.P., Barnett, M.H., Parratt, J.D., Prineas, J.W., 2009. Multiple sclerosis: distribution of inflammatory cells in newly forming lesions. Ann. Neurol. 66, 739–753.

Jenkinson, M., Bannister, P., Brady, M., Smith, S., 2002. Improved optimization for the robust and accurate linear registration and motion correction of brain images. NeuroImage 17, 825–841.

Jenkinson, M., Smith, S., 2001. A global optimisation method for robust affine registration of brain images. Med. Image Anal. 5, 143–156.

Kitzler, H.H., Su, J., Zeineh, M., Harper-Little, C., Leung, A., Kremenchutzky, M., Deoni, S.C., Rutt, B.K., 2012. Deficient MWF mapping in multiple sclerosis using 3D whole-brain multi-component relaxation MRI. NeuroImage 59, 2670–2677.

Kitzler, H.H., Wahl, H., Eisele, J.C., Kuhn, M., Schmitz-Peiffer, H., Kern, S., Rutt, B.K., Deoni, S.C.L., Ziemssen, T., Linn, J., 2018. Multi-component relaxation in clinically isolated syndrome: lesion myelination may predict multiple sclerosis conversion. Neuroimage Clin. 20, 61–70.

Köhler, C., Wahl, H., Ziemssen, T., Linn, J., Kitzler, H.H., 2019. Exploring individual multiple sclerosis lesion volume change over time: Development of an algorithm for the analyses of longitudinal quantitative MRI measures. Neuroimage Clin. 21, 101623.

Kolind, S., Matthews, L., Johansen-Berg, H., Leite, M.I., Williams, S.C.R., Deoni, S., Palace, J., 2012. Myelin water imaging reflects clinical variability in multiple sclerosis. NeuroImage 60, 263–270.

Kuhlmann, T., Miron, V., Cui, Q., Wegner, C., Antel, J., Brück, W., 2008. Differentiation block of oligodendroglial progenitor cells as a cause for remyelination failure in chronic multiple sclerosis. Brain 131, 1749–1758.

Kuhlmann, T., Ludwin, S., Prat, A., Antel, J., Brück, W., Lassmann, H., 2016. An updated histological classification system for multiple sclerosis lesions. Acta Neuropathol. 133, 13–24.

Kutzelnigg, A., 2005. Cortical demyelination and diffuse white matter injury in multiple sclerosis. Brain 128, 2705–2712.

Lassmann, H., van Horssen, J., Mahad, D., 2012. Progressive multiple sclerosis: pathology and pathogenesis. Nat. Rev. Neurol. 8, 647–656.

Patani, R., Balaratnam, M., Vora, A., Reynolds, R., 2007. Remyelination can be extensive in multiple sclerosis despite a long disease course. Neuropathol. Appl. Neurobiol. 33, 277–287.

Patrikios, P., Stadelmann, C., Kutzelnigg, A., Rauschka, H., Schmidbauer, M., Laursen, H., Sorensen, P.S., Brück, W., Lucchinetti, C., Lassmann, H., 2006. Remyelination is extensive in a subset of multiple sclerosis patients. Brain 129, 3165–3172.

Prineas, J.W., Barnard, R.O., Kwon, E.E., Sharer, L.R., Cho, E.S., 1993. Multiple sclerosis: remyelination of nascent lesions. Ann. Neurol. 33, 137–151.

Raine, C.S., Wu, E., 1993. Multiple sclerosis: remyelination in acute lesions. J. Neuropathol. Exp. Neurol. 52, 199–204.

Reich, D.S., White, R., Cortese, I.C., Vuolo, L., Shea, C.D., Collins, T.L., Petkau, J., 2015. Sample-size calculations for short-term proof-of-concept studies of tissue protection and repair in multiple sclerosis lesions via conventional clinical imaging. Multiple Sclerosis J. 21, 1693–1704.

Schmierer, K., Scaravilli, F., Altmann, D.R., Barker, G.J., Miller, D.H., 2004. Magnetization transfer ratio and myelin in postmortem multiple sclerosis brain. Ann. Neurol. 56, 407–415.

Shechter, R., Schwartz, M., 2013. CNS sterile injury: just another wound healing? Trends Mol. Med. 19, 135–143.

Smith, S.M., 2002. Fast robust automated brain extraction. Hum. Brain Mapp. 17, 143–155.

Van Der Valk, P., De Groot, C.J.A., 2000. Staging of multiple sclerosis (MS) lesions: pathology of the time frame of MS. Neuropathol. Appl. Neurobiol. 26, 2–10.

Vargas, W.S., Monohan, E., Pandya, S., Raj, A., Vartanian, T., Nguyen, T.D., Hurtado Rúa, S.M., Gauthier, S.A., 2015. Measuring longitudinal myelin water fraction in new multiple sclerosis lesions. NeuroImage: Clin. 9, 369–375.

Vavasour, I.M., Chang, K.L., Combes, A.J.E., Meyers, S.M., Kolind, S.H., Rauscher, A., Li, D.K.B., Traboulsee, A., MacKay, A.L., Laule, C., 2021. Water content changes in new multiple sclerosis lesions have a minimal effect on the determination of myelin water fraction values. J. Neuroimaging 31, 1119–1125.

Wang, J., Wang, J., Wang, J., Yang, B., Weng, Q., He, Q., 2019. Targeting microglia and macrophages: a potential treatment strategy for multiple sclerosis. Front. Pharmacol. 10, 286.

Yamasaki, R., Lu, H., Butovsky, O., Ohno, N., Rietsch, A.M., Cialic, R., Wu, P.M., Doykan, C.E., Lin, J., Cotleur, A.C., Kidd, G., Zorlu, M.M., Sun, N., Hu, W., Liu, L., Lee, J.C., Taylor, S.E., Uehlein, L., Dixon, D., Gu, J., Floruta, C.M., Zhu, M., Charo, I. F., Weiner, H.L., Ransohoff, R.M., 2014. Differential roles of microglia and monocytes in the inflamed central nervous system. J. Exp. Med. 211, 1533–1549.

Zhang, J., MacKay, A., 2013. Analysing mcDESPOT data with an arbitrary number of T2 components Proc. Intl. Soc. Mag. Reson. Med. 21.